ISSN 2029-6991 / eISSN 2029-7009

VILNIUS TECH
Vilnius Gediminas Technical University

GEODESY and CARTOGRAPHY

2024
Volume 50
Issue 2
Pages 97–103
https://doi.org/10.3846/gac.2024.17720

UDC 528.77:550.814

IDENTIFICATION OF GEOLOGICAL UNITS IN ALBORZ MOUNTAIN IN IRAN USING LANDSAT-9 IMAGE

Komeil ROKNI[1]✉, Davood AKBARI[2]

[1]*Department of Geomatic Engineering, Faculty of Engineering, Gonbad Kavous University, Golestan, Iran*
[2]*Department of Geomatic Engineering, Faculty of Engineering, University of Zabol, Zabol, Iran*

Article History:
- received 01 October 2022
- accepted 20 May 2024

Abstract. In the present study, the suitability of principal components analysis (PCA) based techniques was evaluated for identification of geological units from Landsat-9 satellite imagery. In this respect, a scene of Landsat-9 operational land imager 2 (OLI–2) data of the year 2023 was acquired and a geological map scale 1:100000 of the study area was used as the reference. The results indicated suitability of the PCA based techniques for discrimination of geological units from Landsat-9 image, especially the PCA of decorrelation stretch (DS) approach. The PCA-DS approach, which considered the advantages of both PCA and DS techniques, successfully identified all the geological units in the study area, including the Basalt, Sandstone, Dolomite, and Conglomerate. However, the performance of the PCA and DS techniques was also reasonable for this purpose. On the other hand, the study revealed weak performance of the minimum noise fraction (MNF) and PCA-MNF techniques for geological mapping using Landsat-9 imagery. In conclusion, the study demonstrated the advantage of the PCA-DS approach for geological mapping using Landsat-9 imagery; therefore, it may be useful in futures studies for geological mapping along the whole Alborz Mountain with similar lithological and geomorphological conditions.

Keywords: Landsat-9, principal component analysis, geological mapping.

✉Corresponding author. E-mail: ***rokni@gonbad.ac.ir***

1. Introduction

Geologic mapping is a scientific process that is able to produce a variety of maps for different applications, including evaluating quality of ground waters and contamination risks; land-use planning and land management; forecasting volcano, earthquake, and landslide hazards; describing energy and mineral resources as well as their extraction costs; general education; and waste repository locating (Compton, 1985; Soller, 2002). It is defined as the process of physically going to the field observation and recording the geological information from the rocks that outcrop at the earth surface. The information that usually the geologists looks for are including: the boundaries between different structures and rock types, for example fault-lines and evidence of the rocks undergoing deformation (Davis et al., 2011).

A powerful tool to improve the process of geological mapping is remote sensing (Varnes, 1974; Bernknopf, 1993; Pour & Hashim, 2015; Yang et al., 2018). Remote sensing technology is useful for the explorations of minerals and geothermal energy, geological investigations, and assessment for environmental geology and geotechnical engineering. It is also an essential tool for understanding the significant natural hazards pertinent to geology such as earthquakes, avalanches, floods, river channel migration and avulsion, landslides and debris flows, liquefaction, subsidence, sinkholes, tsunamis, and volcanoes (Bhan & Krishnanunni, 1983). Several image processing techniques have been presented in recent decades for purpose of geological mapping using remote sensing technology, such as band ratio (Inzana et al., 2003), correlation coefficient (Kühn et al., 2009), principal component analysis (PCA) (Loughlin, 1991), minimum noise fraction (MNF) (Fal et al., 2019), decorrelation stretch (DS) (Kenea, 1997), and log residual (Hook et al., 1992) etc.

In this study, the applicability of PCA-based image processing techniques including the PCA, PCA-DS, and PCA-MNF was evaluated for identification of geological units in the study area from Landsat-9 Operational Land Imager 2 (OLI–2) data. The suitability of Landsat image for geological applications is mainly due to the spectral band characteristics of this image, consequently, possibility to perform different image processing techniques for mapping geological units. It was demonstrated in many studies

during the recent decades (Pournamdari et al., 2014; Abdelouhed et al., 2022).

2. Material and methods

2.1. Study area and dataset

The test site is located in north eastern Iran in the Semnan province. The region is surrounded by the mountains and foothills of the North Alborz Mountains that is belonging to the Alp-Himalaya orogenic belt. The active morph dynamics in this region are mainly driven by Aeolian and fluvial activities; the one named last concentrate on the winter half year (Ullmann et al., 2016). This region is covered by concrete layers such as Cretaceous formations, as well as sandstone and Paleogene-related conglomerates. In this area, the unconfined aquifer and bedrock consist of Neogene alluvium, such as marl and conglomerate, and the well logs set out the type of sediment (Arabameri et al., 2019). Location of the study area is displayed in Figure 1.

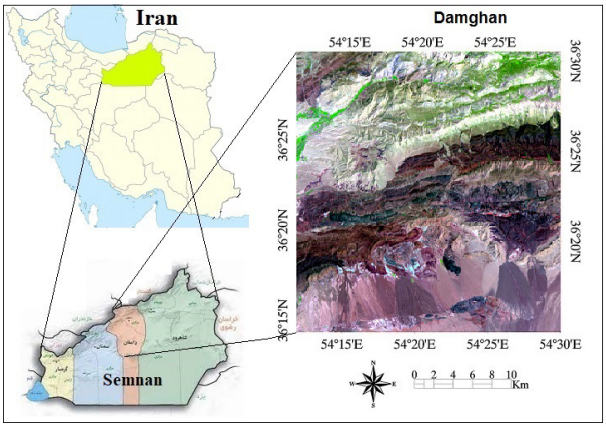

Figure 1. Location of the study area

To carry out discrimination of the geological units in the study area using image processing techniques, one scene of Landsat-9 Operational Land Imager 2 (OLI–2) Collection 2 Level-2 Science Products (L2SP) data acquired in July 2023 was obtained from the US Geological Survey (USGS) Global Visualization Viewer. The L2SP include surface reflectance and surface temperature scene-based products. The acquired Landsat image was pre-georeferenced to north-up UTM projection using WGS-84 datum. Table 1 present the specifications of Landsat data used in this study.

2.2. Geological mapping techniques

The effectiveness of several image processing techniques including the PCA, PCA-DS, and PCA-MNF was evaluated for discrimination of geological units in the study area from Landsat-9 satellite image. A standard principal components analysis (PCA) transformation was applied to Landsat-9 image of the study area. This technique was applied on Landsat visible, near infrared and shortwave infrared bands because of their suitability to extract geological units (Rokni et al., 2011; Pournamdari et al., 2014). A total of seven new image components were created from the Landsat-9 spectral bands. After analysing the eigenvalues we noticed that the first three PCs (PC1, PC2, and PC3) contained total variances, therefore PC1PC2PC3 band combination was used for geological mapping in this study.

In addition, principal components analysis of decorrelation stretch (PCA-DS) was performed for geological mapping. DS is useful to remove high correlation that commonly found in multispectral images and is also appropriate to generate a more colourful composite image for purpose the visualization for improving image interpretation (Gillespie et al., 1998). DS technique was widely used for ophiolite mapping in previous studies (Kenea, 1997; Khan et al., 2007; Seleem et al., 2020). In this study, the PCA technique was applied to transform the achieved DS image into a new PCA space. The resulting PCA-DS image was evaluated for geological mapping.

Furthermore, principal components analysis of minimum noise fraction (PCA-MNF) was implemented. MNF is a noise reduction process that is useful to increase the signal-to-noise ratio in multispectral satellite images. The algorithm of MNF consists of two consecutive rotations of PCA. The first rotation uses the noise covariance matrix to decorrelate and resize the noise in the satellite image. Therefore the noise has a unit variance and no band-to-band correlation. The second rotation uses the PCs which were derived from the result of the first rotation. The data space is divided into two parts. One part is associated with large eigenvalues and coherent Eigen images and another part with near-unity eigenvalues and noise-dominated images (Green et al., 1988).

2.3. Reference map

A geological map scale 1:100000 was used as the reference to evaluate applicability of the applied image processing techniques for discrimination of different geological units

Table 1. Specifications of the Landsat-9 image used in this study

Satellite	Sensor	Year	Resolution (m)	Description
Landsat-9	OLI-2	2023	30	Band 1 Visible Coastal Aerosol (0.43–0.45 μm)
			30	Band 2 Visible Blue (0.450–0.51 μm)
			30	Band 3 Visible Green (0.53–0.59 μm)
			30	Band 4 Red (0.64–0.67 μm)
			30	Band 5 Near-Infrared (0.85–0.88 μm)
			30	Band 6 SWIR 1(1.57–1.65 μm)
			30	Band 7 SWIR 2 (2.11–2.29 μm)
			15	Band 8 Panchromatic (PAN) (0.50–0.68 μm)
			30	Band 9 Cirrus (1.36–1.38 μm)

in the study area from ASTER imagery. This geological map is displayed in Figure 2.

3. Results and discussion

Initially, the DS and MNF techniques were performed to visually identify geological units in the study area from Landsat-9 image. With reference to the geology map of the study area (Figure 2), our inspection indicated that some of the geological units in the study region including the Basalt, Sandstone, Conglomerate, and Dolomite can be discriminated using the DS and MNF techniques. However, as shown in Figure 3, the DS technique well highlighted the geological units from the Landsat-9 image, but MNF could not provide reasonable result for this purpose, especially in identifying Sandstone and Basalt (Figure 4).

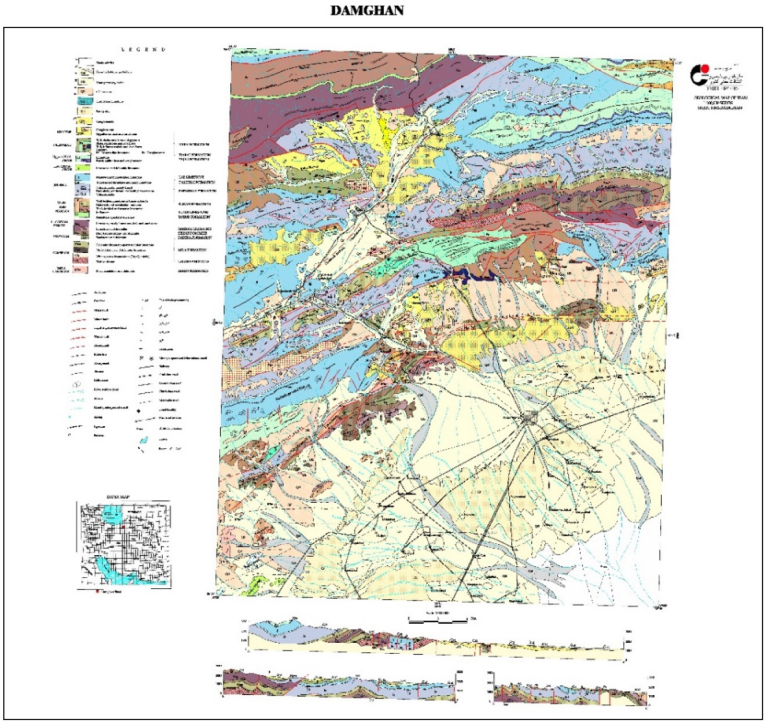

Figure 2. Geological map of the study area

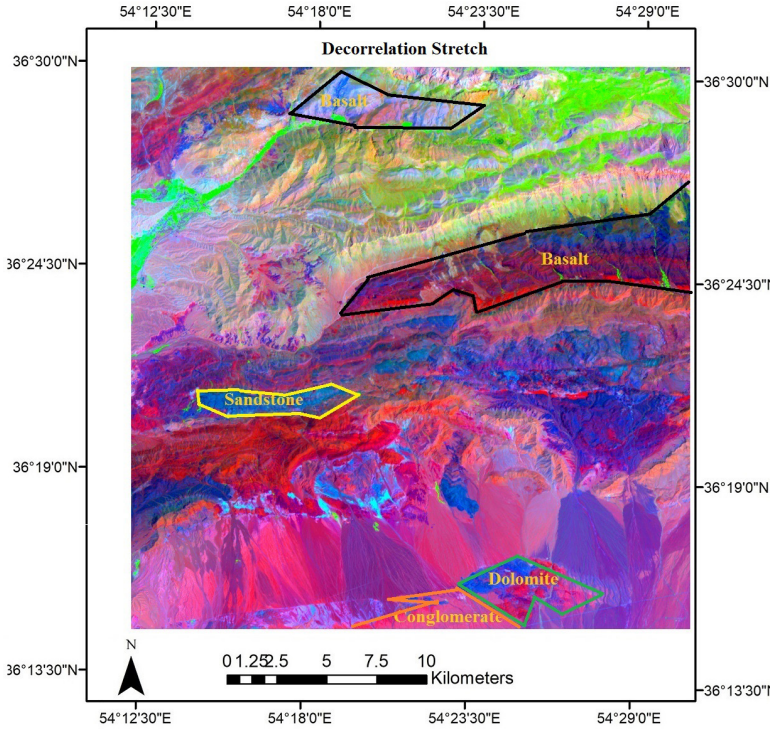

Figure 3. Decorrelation stretch image obtained from Landsat-9 image

Subsequently, the PCA, PCA-DS, and PCA-MNF techniques were implemented to find out their applicability in highlighting different geological units from the Landsat-9 imagery of the study area. After applying the PCA technique on Landsat-9 image, the first three PCs (containing total variances) were selected and evaluated for geological mapping. The result indicated that the PC1, PC2, and PC3 band combination was appropriate to identify Basalt, Sandstone, Conglomerate, and Dolomite from Landsat-9 image of the study area (Figure 5). However, discrimination

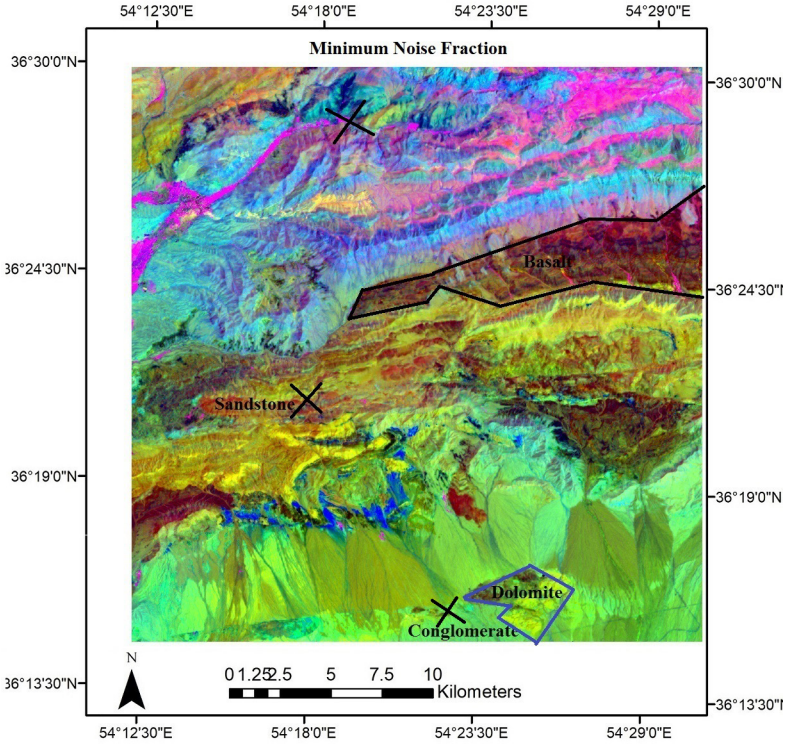

Figure 4. Minimum noise fraction image obtained from Landsat-9 image

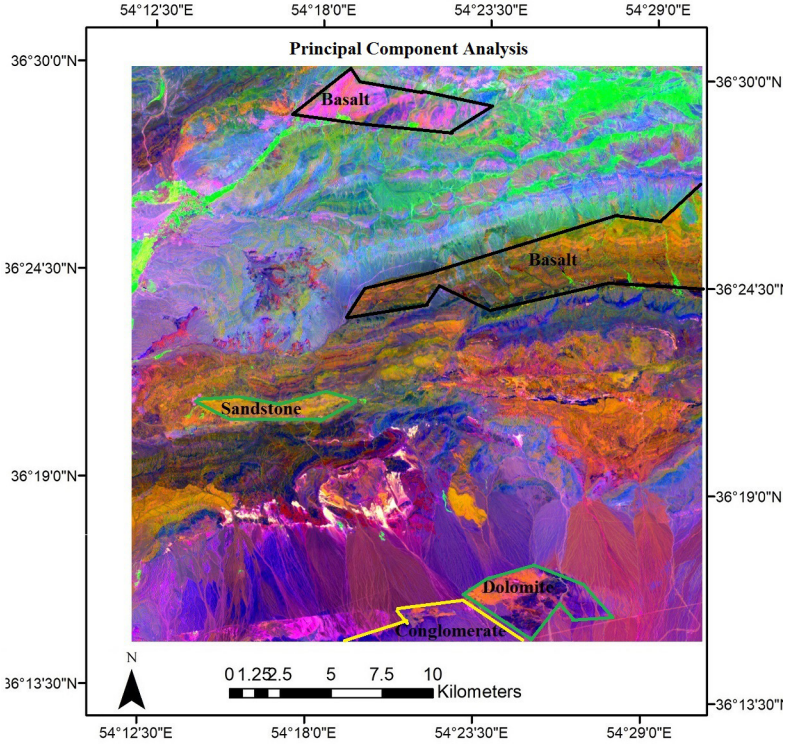

Figure 5. Principal component analysis image obtained from Landsat-9 image

between Basalt and Sandstone was difficult in the outcome PCA image.

Furthermore, as shown in Figure 6, the results revealed that applying the PCA on MNF technique, could not improve the MNF to highlight geological units from Landsat-9 image of the study area. Therefore, both MNF and PCA-MNF techniques were not suitable for geological mapping in this study. Finally, the outcome of PCA-DS was investigated (Figure 7). This approach incorporated the advantages of both PCA and DS techniques. The results

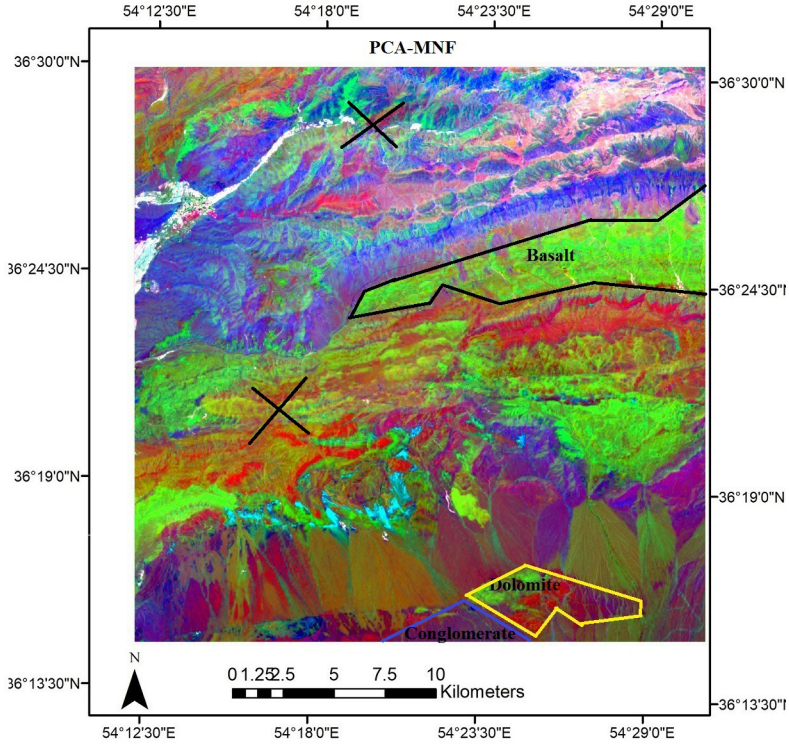

Figure 6. Principal component analysis of minimum noise fraction

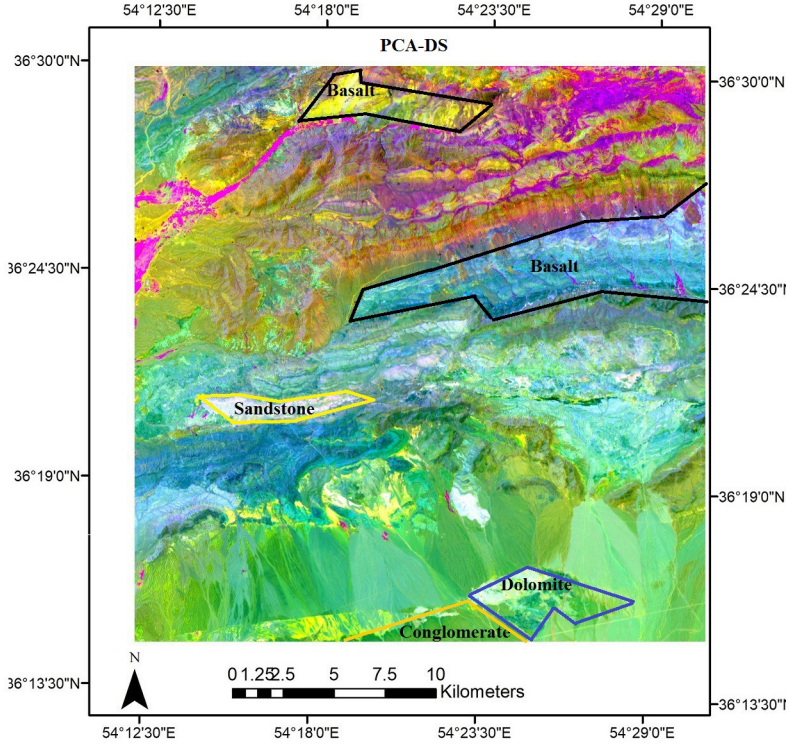

Figure 7. Principal component analysis of decorrelation stretch

indicated that the PCA-DS approach greatly discriminated Sandstone from the Basalt, where Dolomite and Conglomerate units are also observable in the image. Therefore, we recommend this approach for visualizing geological units using Landsat-9 imagery.

Overall, as presented in Table 2, the findings of this study indicated that the identification of Dolomite and Basalt from the Landsat-9 image at the region of Alborz Mountain was easier, so that all the applied techniques were able to partially or totally extract them. The DS, PCA, and PCA-DS approaches highlighted all the geological units in the study area, however, the PCA-DS approach which considered the advantages of both PCA and DS techniques provided a superior output for geological mapping. In contrast, the MNF and PCA-MNF techniques were not successful for this purpose.

Table 2. Performance of the applied techniques in discrimination of geological units

Techniques	Conglomerate	Sandstone	Dolomite	Basalt
DS	√	√	√	√
MNF	×	×	√	√
PCA	√	√	√	√
PCA-MNF	√	×	√	√
PCA-DS	√	√	√	√

4. Conclusions

In this study, the suitability of minimum noise fraction (MNF), decorrelation stretch (DS), principal components analysis (PCA), PCA-DS, and PCA-MNF techniques was evaluated for identifying geological units from Landsat-9 satellite imagery in southern margin of Alborz Mountain in Iran. The results indicated great performance of the PCA-DS approach, which considered the advantages of both PCA and DS techniques, for geological mapping. In addition, the results revealed that the applicability of PCA and DS techniques was also reasonable in discrimination of geological units from Landsat-9 imagery of the study area. On the other hand, the MNF and PCA-MNF techniques were not successful for this purpose. The study concluded that the PCA, DS, and PCA-DS approaches may be useful in futures studies for geological mapping along the whole Alborz Mountain with similar lithological and geomorphological conditions.

Acknowledgements

This work was supported by Gonbad Kavous University through (Grant No. 6/567).

Author contributions

The first author contributed in study conception and design, analysis and interpretation of the results, and manuscript preparation. The second author contributed in data collection, and conceiving and designing the analysis, and English revision.

Declarations

The authors declare no conflict of interest.

References

Abdelouhed, F., Ahmed, A., Abdellah, A., Mohammed, I., & Zouhair, O. (2022). Extraction and analysis of geological lineaments by combining ASTER-GDEM and Landsat 8 image data in the central high atlas of Morocco. *Natural Hazards*, *111*(2), 1907–1929. https://doi.org/10.1007/s11069-021-05122-9

Arabameri, A., Roy, J., Saha, S., Blaschke, T., Ghorbanzadeh, O., & Tien Bui, D. (2019). Application of probabilistic and machine learning models for groundwater potentiality mapping in Damghan Sedimentary Plain, Iran. *Remote Sensing*, *11*(24), Article 3015. https://doi.org/10.3390/rs11243015

Bernknopf, R. L. (1993). *Societal value of geologic maps*. USGS Circular 1111. https://doi.org/10.3133/cir1111

Bhan, S. K., & Krishnanunni, K. (1983). Applications of remote sensing techniques to geology. *Proceedings of the Indian Academy of Sciences Section C: Engineering Sciences*, *6*(4), 297–311. https://doi.org/10.1007/BF02881136

Compton, R. R. (1985). *Geology in the field*. Wiley.

Davis, G. H., Reynolds, S. J., & Kluth, C. F. (2011). *Structural geology of rocks and regions*. John Wiley & Sons.

Fal, S., Maanan, M., Baidder, L., & Rhinane, H. (2019). The contribution of Sentinel-2 satellite images for geological mapping in the south of Tafilalet basin (Eastern Anti-Atlas, Morocco). *The International Archives of Photogrammetry, Remote Sensing and Spatial Information Sciences*, *42*, 75–82. https://doi.org/10.5194/isprs-archives-XLII-4-W12-75-2019

Gillespie, A., Rokugawa, S., Matsunaga, T., Cothern, J. S., Hook, S., & Kahle, A. B. (1998). A temperature and emissivity separation algorithm for Advanced Spaceborne Thermal Emission and Reflection Radiometer (ASTER) images. *IEEE Transactions on Geoscience and Remote Sensing*, *36*, 13–26. https://doi.org/10.1109/36.700995

Green, A. A., Berman, M., Switzer, P., & Craig, M. D. (1988). A transformation for ordering multispectral data in terms of image quality with implications for noise removal. *IEEE Transactions on Geoscience and Remote Sensing*, *26*(1), 65–74. https://doi.org/10.1109/36.3001

Hook, S. J., Gabell, A. R., Green, A. A., & Kealy, P. S. (1992). A comparison of techniques for extracting emissivity information from thermal infrared data for geologic studies. *Remote Sensing of Environment*, *42*(2), 123–135. https://doi.org/10.1016/0034-4257(92)90096-3

Inzana, J., Kusky, T., Higgs, G., & Tucker, R. (2003). Supervised classifications of Landsat TM band ratio images and Landsat TM band ratio image with radar for geological interpretations of central Madagascar. *Journal of African Earth Sciences*, *37*(1–2), 59–72. https://doi.org/10.1016/S0899-5362(03)00071-X

Kenea, N. H. (1997). Improved geological mapping using Landsat TM data, Southern Red Sea Hills, Sudan: PC and IHS decorrelation stretching. *International Journal of Remote Sensing*, *18*(6), 1233–1244. https://doi.org/10.1080/014311697218386

Khan, S. D., Mahmood, K., & Casey, J. F. (2007). Mapping of Muslim Bagh ophiolite complex (Pakistan) using new remote sensing, and field data. *Journal of Asian Earth Sciences*, *30*(2), 333–343. https://doi.org/10.1016/j.jseaes.2006.11.001

Kühn, J., Brenning, A., Wehrhan, M., Koszinski, S., & Sommer, M. (2009). Interpretation of electrical conductivity patterns by soil properties and geological maps for precision agriculture. *Precision Agriculture*, *10*(6), 490–507. https://doi.org/10.1007/s11119-008-9103-z

Loughlin, W. P. (1991). Principal component analysis for alteration mapping. *Photogrammetric Engineering and Remote Sensing*, *57*(9), 1163–1169.

Pour, A. B., & Hashim, M. (2015). Structural mapping using PALSAR data in the Central Gold Belt, Peninsular Malaysia. *Ore Geology Reviews*, *64*, 13–22. https://doi.org/10.1016/j.oregeorev.2014.06.011

Pournamdari, M., Hashim, M., & Pour, A. B. (2014). Application of ASTER and Landsat TM data for geological mapping of esfandagheh ophiolite complex, Southern Iran. *Resource Geology*, *64*(3), 233–246. https://doi.org/10.1111/rge.12038

Rokni, K., Marghany, M., Hashim, M., & Hazini, S. (2011, December). Comparative statistical-based and color-related pan sharpening algorithms for ASTER and RADARSAT SAR satellite data. In *2011 IEEE International Conference on Computer Applications and Industrial Electronics (ICCAIE)* (pp. 618–622). IEEE. https://doi.org/10.1109/ICCAIE.2011.6162208

Seleem, T., Hamimi, Z., Zaky, K., & Zoheir, B. (2020). ASTER mapping and geochemical analysis of chromitite bodies in the Abu Dahr ophiolites, South Eastern Desert, Egypt. *Arabian Journal of Geosciences*, *13*(15), 1–21. https://doi.org/10.1007/s12517-020-05624-z

Soller, D. R. (2002). *Digital Mapping Techniques '02-Workshop Proceedings*. USGS Open-file Report 02-370. U.S. Department of the Interior, U.S. Geological Survey.

Ullmann, T., Büdel, C., Baumhauer, R., & Padashi, M. (2016). Sentinel-1 SAR data revealing fluvial morphodynamics in damghan (Iran): Amplitude and coherence change detection. *International Journal of Earth Science and Geophysics*, *2*(1). https://doi.org/10.35840/2631-5033/1807

Varnes, D. J. (1974). *The logic of geological maps, with reference to their interpretation and use for engineering purposes*. USGS Professional Paper 837. United States Government Printing Office. https://doi.org/10.3133/pp837

Yang, M., Ren, G., Han, L., Yi, H., & Gao, T. (2018). Detection of Pb–Zn mineralization zones in west Kunlun using Landsat 8 and ASTER remote sensing data. *Journal of Applied Remote Sensing*, *12*(2), Article 026018. https://doi.org/10.1117/1.JRS.12.026018